2011-01-01

Experimental Demonstration of an All-Fiber Variable Optical Attenuator Based on Liquid Crystal Infiltrated Photonic Crystal Fiber

Sunish Mathews
Dublin Institute of Technology

Gerald Farrell
Dublin Institute of Technology, gerald.farrell@dit.ie

Yuliya Semenova
Dublin Institute of Technology, yuliya.semenova@dit.ie

Recommended Citation

Mathews, S., Farrell, G. &Semenova, Y. (2011) Experimental Demonstration of an All-Fiber Variable Optical Attenuator Based on Liquid Crystal Infiltrated Photonic Crystal Fiber. *Microwave and Optical Technology Letters,*Vol.53, no. 3, pp. 539–543. doi:10.1002/mop.25789

Experimental Demonstration of an All-Fiber Variable Optical Attenuator based on Liquid Crystal Infiltrated Photonic Crystal Fiber

Sunish Mathews, Gerald Farrell, Yuliya Semenova

Photonics Research Centre

School of Electronic and Communications Engineering

Dublin Institute of Technology

Kevin Street, Dublin 8

Ireland

ABSTRACT:

The application of a nematic liquid crystal infiltrated solid core Photonic Crystal Fiber as a novel all-fiber in-line electronically controlled broadband fiber optic attenuator in the wavelength range from 1500 nm – 1600 nm is demonstrated. The device based on photonic bandgap transmission, is electronically controlled and due to its compact configuration, can be easily incorporated into an optical network. A low insertion loss at zero attenuation state and a high extinction ratio of ~ 40 dB is obtained between the high and low transmission states of the attenuator. The device works on the application of a varying voltage applied perpendicular to the fiber axis. The attenuation varies linearly with an increase in voltage, with a ~ 3.5 V increment required for 1 dB attenuation. The device is shown to have a flat spectral response for all attenuation states in the wavelength range. The device can be used as the core of a highly efficient in-line electronically controlled variable fibre optic attenuator.

Keywords:

Photonic Crystal Fibers, Liquid Crystal Infiltration, Photonic Bandgap Transmission, Variable Optical Attenuator, In-Fiber Tunable Devices.

1. INTRODUCTION

Photonic crystal fibers (PCFs) in recent years have attracted considerable interest due to their novel light guidance properties. With a cross-sectional microstructure geometry which can be modified during the fabrication stage, control of the optical and propagation properties of a PCF is possible. The propagation properties of PCFs can also be dynamically tuned by filling the air-holes with materials whose refractive indices can be easily varied by external physical fields [1]. This advantage of PCFs makes them highly desirable for the fabrication of in-fiber tunable devices.

Liquid crystal (LC) materials with their high dielectric anisotropy ($\Delta\varepsilon \sim 70$) and high birefringence ($\Delta n \sim 0.6$) are good candidates for infiltration of PCFs air-holes, in order to achieve tunability of light propagation properties. Liquid crystal (LC) materials possess very high thermo-optic and electro-optic coefficients and on infiltration into PCFs they allow for the thermal and electronic tuning. The light guidance in solid-core PCF switches from modified total internal reflection to photonic bandgap (PBG) guidance on infiltration with nematic liquid crystals (NLCs). So far, various in-fiber tunable devices based on PBG guidance have been demonstrated which employ thermal and electronic tuning of the LC infiltrated PCFs [2-5]. The electronic tunability of nematic liquid crystal (NLC) infiltrated solid-core PCF has been studied extensively for in-fiber tunable device applications such as a broadband polarizer [6] and very recently a gain equalization filter by employing frequency tunability of a nanoparticle doped NLC infiltrated PCF [7]. Continuous control of the spectral positions of PCF bandgaps has been demonstrated in various all-fiber and in-line device applications by employing the electronic tunability of dual frequency infiltrated PCF [8].

Variable optical attenuators (VOAs) are widely used in optical networks for control of optical power levels in network channels, for example to ensure that the output power level to a receiver is always less than the overload threshold for the receiver, regardless of the optical path loss. There have been various approaches used for fabricating VOAs such as, opto-mechanical systems, micro electromechanical systems (MEMS), planar lightguide circuits (PLC) and thermo-optic methods [9-11]. These have the disadvantages of slow response time due to mechanical or thermal control, the difficulty of integration with other optical devices and high manufacturing costs. VOAs based on LC [12] particularly Polymer dispersed liquid crystals (PDLC) [13, 14] have been studied in detail, however these employ complex system configurations utilising free-space optics which increases cost and induces high insertion losses. Robustness, compact size and low cost are necessary requirements for VOAs in optical networks. An all-fiber configuration for a VOA solves the interface problem between a VOA and a single mode fiber (SMF), ensuring low insertion loss and negligible back reflections.

In this paper, we demonstrate a novel application of nematic liquid crystal infiltrated solid core photonic crystal fiber as an in-line variable optical attenuator in the wavelength range 1500 nm – 1600 nm. The device has a simple and compact all-fiber configuration. The device possesses a low insertion loss (< 1 dB), can achieve ~ 40 dB attenuation and has a flat spectral response for all attenuation levels over the entire wavelength range. The attenuation level of the device is electronically controlled by the amplitude of a square wave voltage applied in a direction perpendicular to the infiltrated fiber axis. The attenuation varies linearly with the applied voltage over a range from 170 Vpp to 310 Vpp. The device is shown to have a response time of the order of milliseconds.

2. PRINCIPLE OF OPERATION

A solid core PCF guides light by modified total internal reflection. When the air-holes of the solid core PCF are infused with NLC, the holey cladding region of the fiber assumes the effective refractive index of the NLC which is higher than the core. Guidance in such fibers is due to multiple reflections from the high-index material and silica interfaces which results in transmission within a number of wavelength intervals allowed by the Photonic Bandgaps (PBGs) formed by the 2-dimensional cross-sectional periodic structure of the PCF [2].

NLC molecules within the holes of the PCF mostly align along the fiber axis without any pre-treatment of the inner surface of the holes. On the application of an electric field the LC molecules undergo reorientation within the holes above a threshold voltage referred to as the Frederiks transition threshold [15]. Below this voltage the propagation properties are governed by the ordinary refractive index of the LC and there is long range orientation order of the LC molecules with alignment along the axis of the fiber. Above the threshold the LC molecules reorient themselves along the direction of the applied field and the propagation is governed by the effective refractive index, which is partially set by the extraordinary refractive index of the NLC. As the LC molecules begin to reorient under the action of the electric field, there is loss in the long range orientation order of the LC within the PCF holes in the cladding region. This causes disturbance of the propagation conditions as light is coupled into the cladding and in effect there is a gradual decrease in the power transmitted through the core of the LC infiltrated PCF.

3. EXPERIMENTAL SETUP

The fiber used for this study is the LMA-10 (Crystal Fibre A/S, Denmark) solid core PCF. The high-index solid core has a diameter of ~ 10 μm, which is surrounded by seven rings of air holes arranged in a triangular lattice. The hole diameter is ~ 3.0 μm and the inter-hole spacing is ~ 7.0 μm while the cladding diameter is ~ 125 μm. The nematic liquid crystal mixture used to infiltrate the fiber is 5CB (Merck Ltd), which has a nematic phase at 22.5 – 35.5°C and becomes isotropic at temperatures higher than 35°C. The ordinary and extraordinary refractive indices of the NLC are ~ 1.52 and ~ 1.71 evaluated at 1550 nm using the Cauchy's relations.

A section of the LMA-10 fiber was used and one end was initially spliced to an SMF28 pigtail using a standard fusion splicer. The splice loss was minimised by optimising the splicing conditions to achieve minimal PCF air-hole collapse at the splice joint. This is done by setting an appropriate fusion time and fusion current [16]. The open end of the PCF was infiltrated with the NLC by immersing the cleaved end of the fiber into a drop of 5CB kept at room temperature. The NLC is drawn into the PCF air-holes due to capillary action and an infiltration length of ~ 2.4 cm was achieved. The infiltrated end was observed under a polarising microscope to ascertain the quality of infiltration, before subjecting it to the electric field to study the attenuation properties.

The experimental set-up to study the electronic tunability and attenuation properties of the infiltrated PCF is as shown in Figure 1. The infiltrated end was placed between two electrodes to allow the application of an electric field in a direction perpendicular to the fiber axis. The electric field was provided by a square wave voltage applied to the PCF using a waveform generator and a voltage amplifier. The light is launched into the PCF

from the spliced end and is collected from the infiltrated end by butt-coupling it to another SMF pigtail using an XYZ nano-positioner stage. We used a broadband source together with an optical spectrum analyser (OSA) to record the spectrum and a tunable laser source together with a high-speed power meter for the attenuation and time response studies.

4. ATTENUATION PROPERTIES OF THE DEVICE

4.1 Spectral Properties of the infiltrated Fiber:

In order to study the spectral properties and attenuation characteristics of the nematic LC infiltrated PCF, a square wave voltage of frequency 1 kHz is applied to the device. Light from the broadband source is transmitted through the infiltrated section of the PCF and the spectrum at different voltages is recorded by the OSA. Figure 2 shows the spectral characteristics of the device in the wavelength range from 1500 nm – 1600 nm with a change in the applied voltage. The spectrum shows a flat response for the entire wavelength range as can be seen from figure 2. For applied voltages from 0 Vpp to 170 Vpp the spectral response of the fiber is that of the source and no bandgaps are observed in the wavelength range. Attenuation of the transmitted intensity is observed from a voltage of ~ 170 Vpp and attains its maximum value at a voltage of ~ 300 Vpp. The NLC molecules undergo continuous reorientation due to the application of the voltage and the optical power transmitted through the core of the PCF reduces and is coupled increasingly into the infiltrated cladding region with an increase in voltage above 170

Vpp. This implies that the NLC molecules align themselves along the electric field direction as voltage increases, in this case perpendicular to the fiber axis.

4.2 Polarization Microscope studies:

A small section less than 1 mm in length of the 5CB infiltrated LMA-10 PCF was observed under a polarising microscope to examine the effect of the applied voltage on the reorientation of the LC molecules. The infiltrated fiber was sandwiched between two ITO coated glass slides to allow the application of the voltage. Figure 3 shows the photographs of the 5CB infiltrated section of the LMA-10 PCF as observed under the polarizing microscope in crossed polarizers mode at three different voltages. The study was performed with visible light transmitted perpendicular to the PCF axis. In the crossed polarizers mode with the axis of the fiber aligned along the polarizer, the infiltrated holey region of the fiber transmits minimum light. This suggests that the LC molecules are mostly aligned along the axis of the fiber within the PCF holes. As the voltage applied to the infiltrated fiber is increased to 170 Vpp, the LC infiltrated region became brighter and a change in colour of the transmitted light is observed. The colour of the transmitted light changed as the voltage was increased further and infiltrated region was the brightest at the maximum voltage of 380 Vpp. The birefringence of the NLC infiltrated holey region of the PCF continuously changes with the applied field above the threshold voltage, this causes the change in colour when observed through the polarization microscope. This observation confirms that LC molecules within the holes begin to reorient under the action of the electric field at a voltage of ~ 170 Vpp and undergo progressive reorientation as the voltage is increased further.

4.3 Linear Attenuation Response of the device:

The attenuation in the voltage range from 170 Vpp to 310 Vpp varies linearly with the increase in voltage. In order to demonstrate this we replaced the broadband source with a tunable laser and measured the transmitted intensity through the device at voltages from 140 Vpp to 310 Vpp in steps of 4 Vpp. Figure 4 shows the transmitted intensity through the fiber at wavelengths 1525 nm, 1550 nm and 1575 nm. As can be seen the attenuation shows a linear response with an increase in voltage in the range from ~ 170-310 Vpp. An extinction ratio of ~ 40 dB is obtained between the high and low transmission states of the device. As expected from figure 2, the spectral response at different voltages showed that the linear response is maintained for the entire wavelength range from 1500 nm – 1600 nm. A linear fit performed with the data at 1550 nm shows that a ~ 3.5 Vpp increment is required to produce an attenuation of 1 dB for the attenuator as shown in figure 5.

4.4 Time response of the device:

The response time of the device was estimated by applying a low frequency (5 Hz) square wave voltage at 300 Vpp to the infiltrated PCF and measuring the output power for time steps ~ 0.05 msec using a high-speed optical power meter at 1550 nm. The switch ON and switch OFF time responses of the device are shown in Figure 8 (a) & (b). The measured values for the ON and OFF times t_{on} and t_{off} are ~ 4 ms and ~ 20 ms respectively, estimated from the time plots as the time taken for the transmittance to change from 90% to 10% and 10% to 90% respectively.

5. CONCLUSIONS

We have experimentally demonstrated the applicability of a nematic liquid crystal infiltrated photonic crystal fiber for use as an electronically controlled in-line all-fiber variable optical attenuator in the wavelength range from 1500 nm – 1600 nm. The device operates on the principle of photonic bandgap guidance and has a low insertion loss and exhibits ~ 40 dB attenuation between its high and low transmission states as a square wave voltage is applied to the NLC infiltrated part of the PCF. The attenuation is linear in the voltage range from 170 Vpp to 310 Vpp and the spectral response of the device for the entire wavelength range is flat for all attenuation states. The attenuator is also shown to have response time in the order of milliseconds. With it's simple all-fiber in-line configuration it has the advantages of ease of optical coupling and interfacing, low insertion loss, as well as low fabrication cost and could be efficiently used for applications in optical networks for optical power level equalization, control and maintenance.

6. REFERENCES

[1] T. Larson, A. Bjarklev, D. Hermann, and J. Broeng, Optical Devices based on liquid crystal photonic bandgap fibres, Opt Exp 11 (2003), 2589-2596.

[2] T. T. Alkeskjold, L. Scolari, D. Noordegraaf, J. Laegsgaard, J. Weirich, L. Wei, G. Tartarini, P. Bassi, S. Gauza, S. T. Wu, and A. Bjarklev, Integrating liquid crystal based optical devices in photonic crystal fibers, Opt Quant Electron 39 (2007), 1009-1019.

[3] T. R. Wolinski, K. Szaniawska, S. Ertman, P. Lesiak, A. W. Domanski, R. Dabrowski, E. N. Kruszelnicki, and J. Wojcik, Influence of temperature and electric fields on propagation properties of photonic liquid crystal fibers, Meas Sci Tech 17 (2006), 985-991.

[4] L. Scolari, T. T. Alkeskjold, and A. Bjarklev, Tunable Gaussian filter based on tapered liquid crystal photonic bandgap fibre, Electron Lett 42 (2006), 1270-1271.

[5] S. Mathews, Y. Semenova, and G. Farrell, Electronic tunability of ferroelectric liquid crystal infiltrated photonic crystal fiber, Electron Lett 45 (2009), 617-618.

[6] T. T. Alkeskjold, and A. Bjarklev, Electrically controlled Broadband Liquid Crystal Photonic Bandgap Fiber Polarimeter, Opt Lett 32 (2007), 1707-1709.

[7] L. Scolari, S. Gauza, H. Xianyu, L. Zhai, L. Eskildsen, T. T. Alkeskjold, S. T. Wu, and A. Bjarklev, Frequency Tunability of solid-core photonic crystal fibers filled with nanoparticle-doped liquid crystals, Opt Exp 17 (2009), 3754-3764.

[8] L. Scolari, T. T. Alkeskjold, J. Riishede, A. Bjarklev, D. S. Hermann, Anawati, M. D. Nielsen, and P. Bassi, Coutinously tunable devices based on electrical control of dual frequency liquid-crsytal filled photonic bandgap fibers, Opt Exp 13 (2005), 7483 – 7496.

[9] M. Morimoto, K. Morimoto, K. Sato, and S. Iizuka, Development of a Variable Optical Attenuator using MEMS Technology, Furukawa Rev 23 (2003), 26-32.

[10] T. Kawai, M. Koga, M. Okunu, and T. Kitoh, PLC-type compact variable optical attenuator for photonic transport network, Electron Lett 34 (1998), 364-365.

[11] P. Qu, W. Chen, F. Li, C. Liu, and W. Dong, Analysis and design of thermo-optical variable optical attenuator using three waveguide directional couplers based on SOI, Opt Exp 16 (2008), 20334-20344.

[12] Y. Q. Lu, F. Du, Y. H. Lin, and S. T. Wu, Variable Optical Attenuator based on polymer stabilized twisted nematic liquid crystal, Opt Exp 12 (2004), 1221-1227.

[13] P. Chanclou, B. Vinouze, M. Roy, C. Cornu, and H. Ramanitra, Phase-shifting VOA with polymer dispersed liquid crystal, J Lightwave Technol 21 (2003), 3471-3476.

[14] K. M. Chen, H. Ren, and S. T. Wu, PDLC based VOA with small polarization dependent loss, Opt Commun 282 (2009), 4374-4377.

[15] M. W. Haakestad, T. T. Alkeskjold, M. D. Nielsen, L. Scolari, J. Riishede, H. E. Engan, and A. Bjarklev, Electrically Tunable Photonic Bandgap Guidance in a Liquid Crystal Filled Photonic Crystal Fiber, Photon Tech Lett 17 (2005), 819-821.

[16] L. Xiao, M. S. Demokan, W. Jin, Y. Wang, C. Zhao, Fusion Splicing Photonic Crystal Fibers and Conventional Single-Mode Fibers: Microhole Collapse Effect, J Lightwave Tech 25 (2007), 3563- 3574.

CAPTIONS FOR FIGURES:

Figure 1: Schematic of the experimental set-up to study the attenuation properties of NLC infiltrated LMA-10 PCF.

Figure 2: 3-D plot showing the spectral response of the 5CB infiltrated LMA-10 PCF in the wavelength range 1500 nm – 1600 nm as the applied voltage is varied from 0 to 380 Vpp at 1 kHz.

Figure 3: Photographs of the LMA-10 PCF sections infiltrated with 5CB as observed under a polarizing microscope at voltages 0 Vpp, 200 Vpp and 370 Vpp at 1 kHz.

Figure 4: Attenuation of the device with increase in voltage from 140 Vpp to 310 Vpp at wavelengths 1525 nm, 1550 nm and 1575 nm. The region of linearity is from 170 Vpp to 310 Vpp.

Figure 5: Linear Response of the attenuation in the voltage range from 170 Vpp to 310 Vpp at 1550 nm, shown with the linear fit for the data.

Figure 6: Time response of the PCF attenuator measured at 1550 nm with a 5 Hz square wave voltage at 300 Vpp (a) Switch ON time response and (b) Switch OFF time response.

Figure 1:

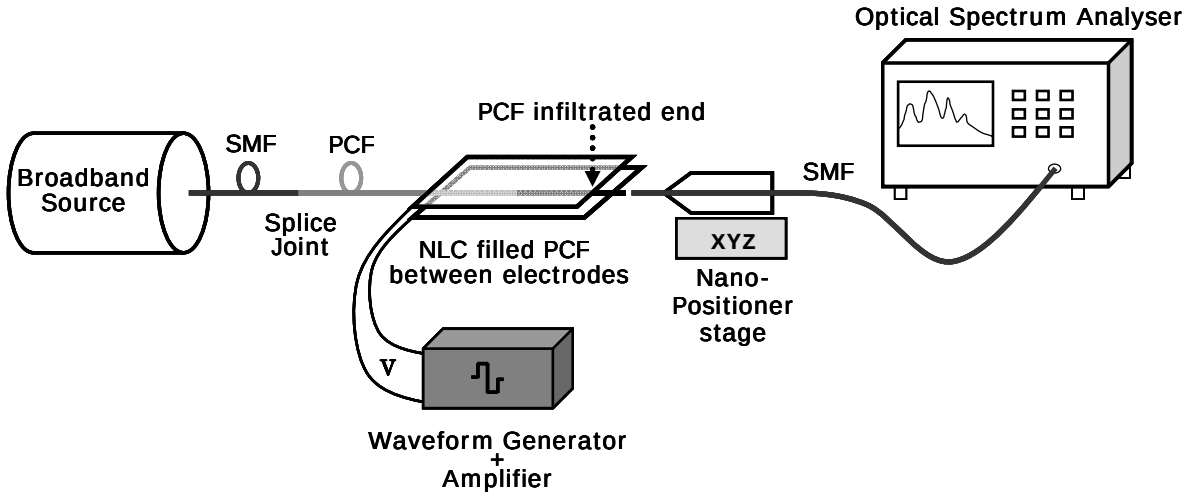
Optical Spectrum Analyser
PCF infiltrated end
Broadband Source
SMF
PCF
Splice Joint
NLC filled PCF between electrodes
SMF
XYZ
Nano-Positioner stage
V
Waveform Generator + Amplifier

Figure 2:

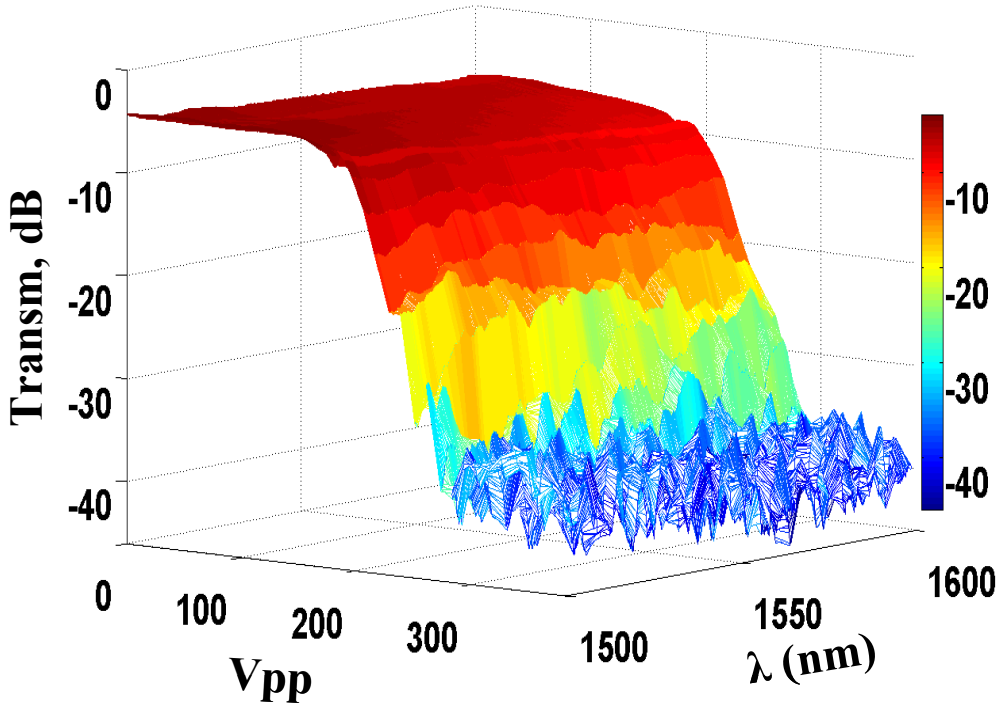
Transm, dB
0
-10
-20
-30
-40
0
100
200
300
Vpp
1500
1550
1600
λ (nm)
-10
-20
-30
-40

Figure 3:

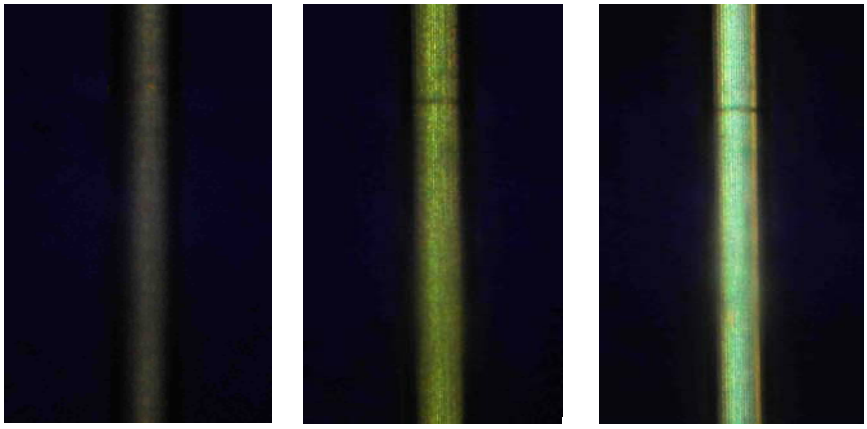

Figure 4:

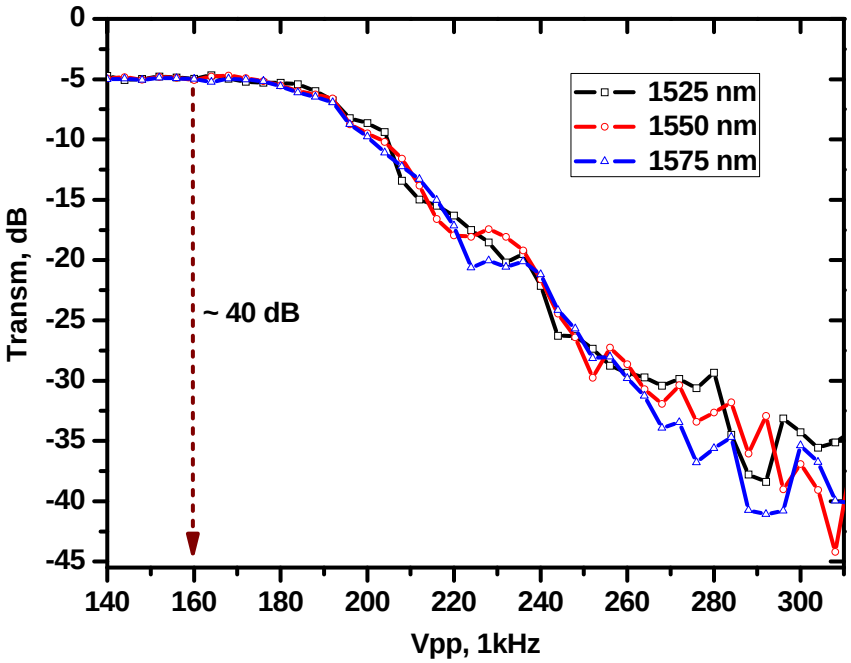
0
-5
-10
-15
-20
-25
-30
-35
-40
-45
Transm, dB
140
160
180
200
220
240
260
280
300
Vpp, 1kHz
~ 40 dB
1525 nm
1550 nm
1575 nm

Figure 5:

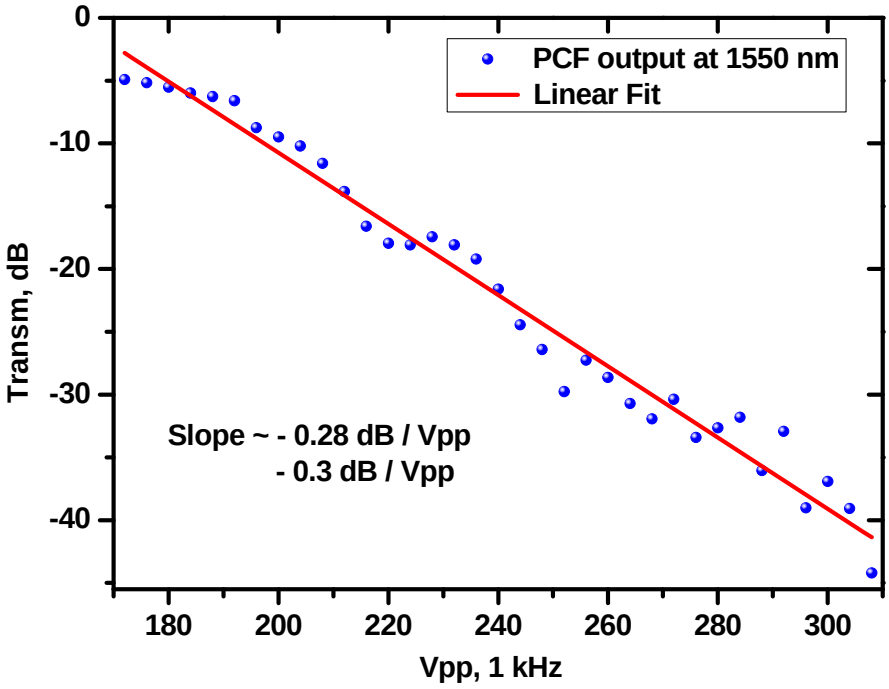
PCF output at 1550 nm
Linear Fit
Slope ~ - 0.28 dB / Vpp
- 0.3 dB / Vpp
Transm, dB
Vpp, 1 kHz
0
-10
-20
-30
-40
180
200
220
240
260
280
300

Figure 6:

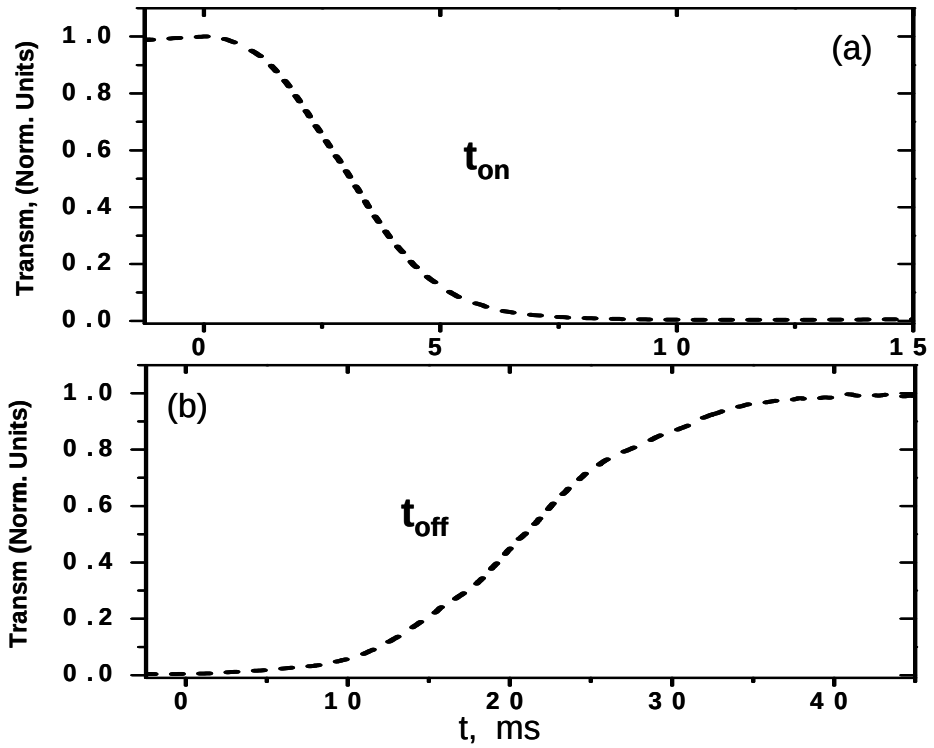
Transm, (Norm. Units)
1.0
0.8
0.6
0.4
0.2
0.0
(a)
t_{on}
0
5
10
15
Transm (Norm. Units)
(b)
t_{off}
0
10
20
30
40
t, ms